Supplementary Information

Pd_3Se_{10}: A Semiconducting Cluster-Based Material

Cullen T. Irvine,[a] Chenguang Wang,[a] Bowen Yu,[b] Tianze Song,[a] Alexander Reifsnyder,[bc] Yehia Khalifa,[a] Wolfgang Windl,[b] David W. McComb,[bc] and Joshua E. Goldberger*[a]

[a]Department of Chemistry and Biochemistry, The Ohio State University, 151 W. Woodruff Ave, Columbus, Ohio 43210, USA

[b] Department of Materials Science and Engineering, The Ohio State University, 140 W 19th Ave, Columbus, Ohio 43210, USA

[c]Center for Electron Microscopy and Analysis, The Ohio State University, 1305 Kinnear Rd, Columbus, Ohio 43212, USA

Table S1. Summary of the tested reaction conditions and PXRD results for the Pd_3Se_{10} syntheses.

Reaction Temperature	Reaction Time	Na_2PdCl_4 Injection Rate	PXRD Result
245 °C	30 s	Fast Addition	Pure Pd_3Se_{10}
245 °C	3 min	Fast Addition	Pd_3Se_{10}, with minor O-$PdSe_2$ impurity
245 °C	10 min	Fast Addition	Pd_3Se_{10}, with minor O-$PdSe_2$ and Se impurities
245 °C	1 h	Fast Addition	Pd_3Se_{10}, with major O-$PdSe_2$ and Se impurities
100 °C	1 h	Fast Addition	Amorphous
150 °C	1 h	Fast Addition	Amorphous
200 °C	1 h	Fast Addition	Pd_3Se_{10}, with Se and unknown impurities
200 °C	10 min	Fast Addition	Pure Pd_3Se_{10}
200 °C	10 min	*Average* of 1.5 mL/min (0.5 mL injection every 20 seconds)	Pure Pd_3Se_{10}
200 °C	1 h	*Average* of 0.25 mL/min (0.25 mL injection every minute)	Pure Pd_3Se_{10}

Notes on reaction temperature: The reaction temperature is the temperature that the $Na_2Se_{3.33}$ solution was heated to before the addition of the Na_2PdCl_4 solution. Since the Na_2PdCl_4 solution was at a lower temperature, its addition results in a decrease in the reaction temperature. For most of the reactions, the solution was then reheated to the desired reaction temperature, where it was maintained for the remainder of the reaction. For very short reactions (30 s and 3 min) with a fast addition of the Na_2PdCl_4 precursor, it was not possible to reheat the solution to the desired reaction temperature before the end of the reaction. When a slow injection rate was used, a consistent reaction temperature (± 5 °C) was easily maintained.

Notes on reaction time: For the slow injection rate experiments, the reaction time includes the entire time it takes to add all of the Na_2PdCl_4 precursor. Once all of the Na_2PdCl_4 precursor had been added for these experiments, the reaction was ended.

Notes on injection rate: "Fast Addition" means that the Na_2PdCl_4 solution was added quickly, and all at once, at the start of the reaction. For the slower injection rate experiments, the Na_2PdCl_4 solution was added manually in 0.25 mL or 0.5 mL portions with a set amount of time in between injections. Since the Na_2PdCl_4 solution was not added continuously, the injection rates are more accurately described as the average rates at which the Pd precursor solution was added.

Rietveld Refinement Plot for the Na_2Se_3 / Na_2Se_4 Precursor

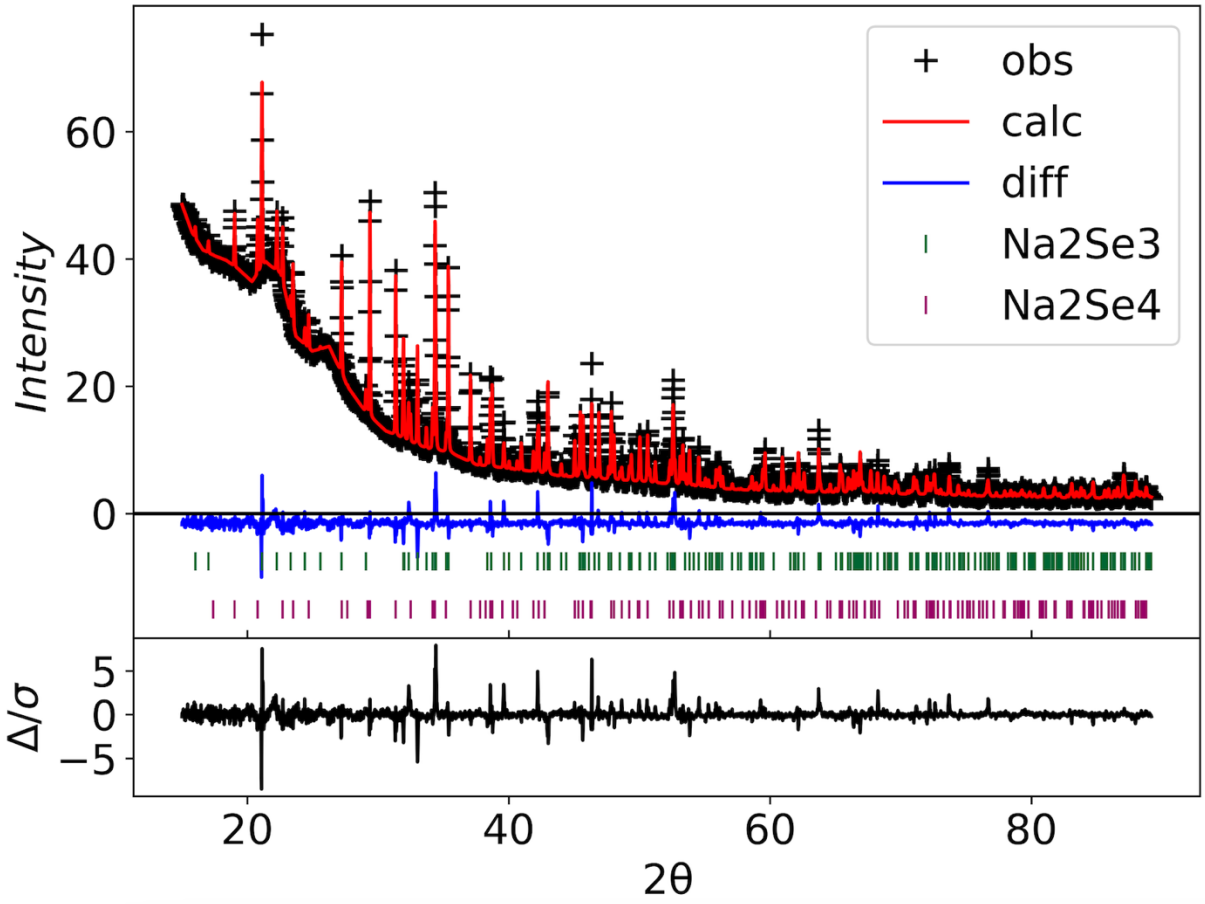

Figure S1. Rietveld refinement of lab powder X-ray diffraction (PXRD) data for the sodium polyselenide precursor consisting of Na_2Se_3 and Na_2Se_4.

Table S2. Phase, weight, and mole fractions for Na_2Se_3 and Na_2Se_4 in the sodium polyselenide precursor. Phase and weight fractions were determined from the refinement of the PXRD data shown in Figure S1. Mole fraction was calculated from weight fraction.

Phase	Na_2Se_3	Na_2Se_4
Phase Fraction	0.779(4)	0.221(4)
Weight Fraction	0.580(5)	0.420(5)
Mole Fraction	0.639(7)	0.361(5)

Crystal Structure of Na_2Se_3

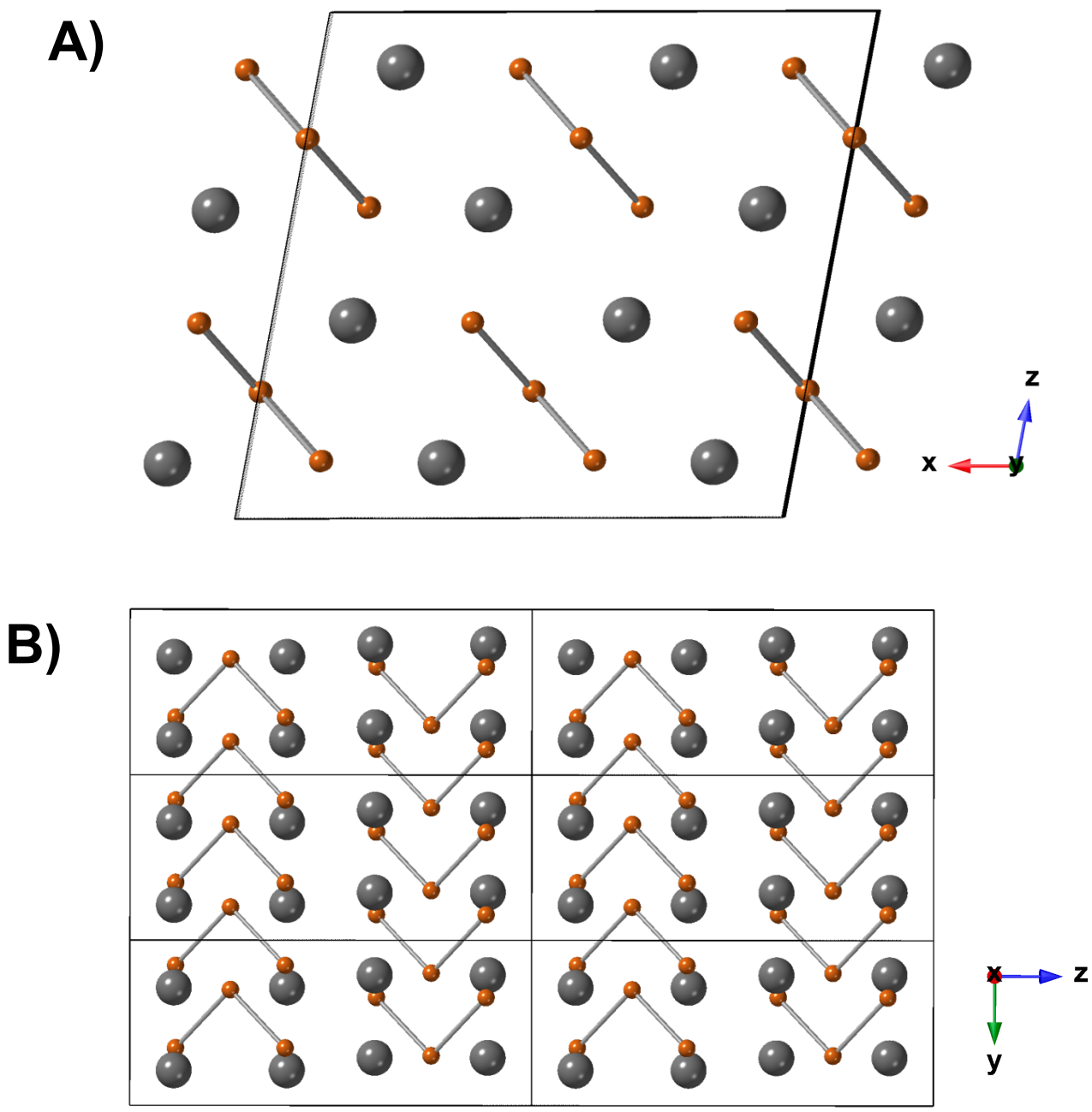

Figure S2. Crystal structure of Na_2Se_3 A) looking down the y-axis and B) looking down the x-axis. Sodium atoms are grey and selenium atoms are orange. The black lines represent the unit cell.

Crystal Structure Data for Na_2Se_3

Table S3. Crystal data for Na_2Se_3 and Rietveld refinement results for the plot in Figure S1.

Chemical Formula	Na_2Se_3
Formula Weight (g/mol)	282.86
Space Group	C2/c
Crystal System	Monoclinic
a (Å)	11.2633(5)
b (Å)	4.27927(10)
c (Å)	10.5986(5)
β (°)	100.8003(18)
Cell Volume (Å^3)	501.791(21)
Z	4
Density (g/cm^3)	3.7442
Sample Temperature (K)	295
Sample Pressure (MPa)	0.1
Lambda (Å)	1.54056
Pattern Range (2θ, degrees)	15.0-89.2
wR	5.277%
GOF	2.34

Table S4. Fractional atomic coordinates and atomic isotropic displacement parameters (U_{iso}) for the refined Na_2Se_3 structure from lab powder X-ray diffraction.

Site	X	Y	Z	Atom	Occupancy	Mult.	U_{iso}
Na (1)	0.3552(9)	0.7124(28)	0.8907(10)	Na	1	8	0.025(4)
Se (1)	0.1352(3)	0.6535(10)	0.3865(4)	Se	1	8	0.0204(13)
Se (2)	0.00000	0.3004(14)	0.25000	Se	1	4	0.0244(21)

Table S5. Bond distances and angles for the Se_3^{2-} anion in alkali metal triselenides.

Alkali Metal Triselenide	Se-Se Bond Distance	Se-Se-Se Bond Angle	Reference
Na_2Se_3	2.423Å	102.827°	**This Work**
K_2Se_3	2.383Å	102.558°	[1]
Rb_2Se_3	2.377Å	103.452°	[2]
Cs_2Se_3	2.354 Å	103.513°	[2]

Pd_3Se_{10} PXRD Patterns for Reactions at 245 °C

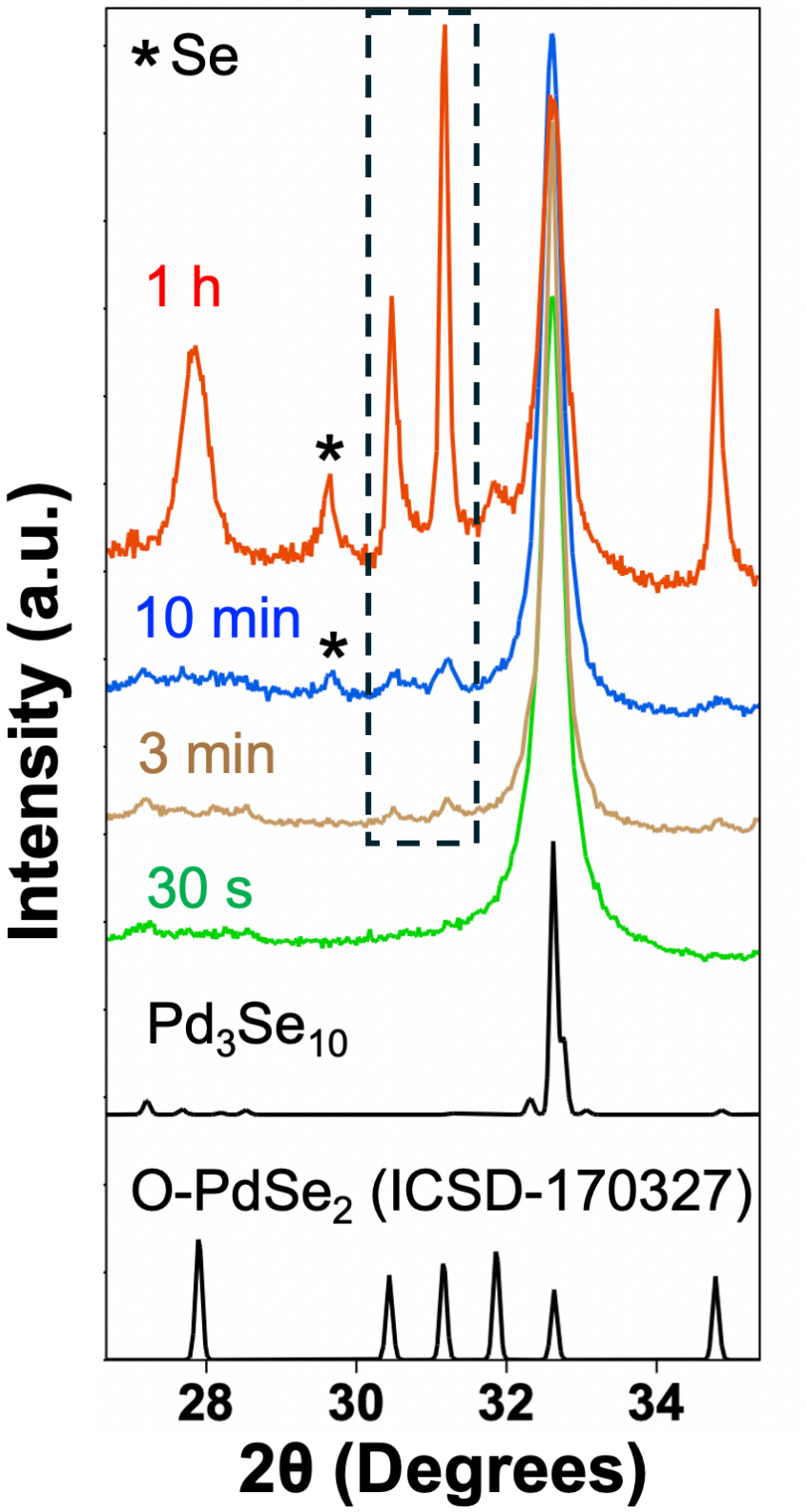

Figure S3. PXRD patterns for the products of the 30 s, 3 min, 10 min, and 1 h reactions performed at 245 °C with a fast addition of the Na_2PdCl_4 precursor. This specific 2θ range was chosen to highlight the low intensity impurity peaks present in some of the samples. The selenium impurity peak is indicated with an asterisk. The dashed line rectangle is highlighting the presence of O-$PdSe_2$ peaks in the 3 min, 10 min, and 1 h samples.

Pd_3Se_{10} PXRD Pattern for the 1-hour, Fast Precursor Addition Reaction at 200 °C

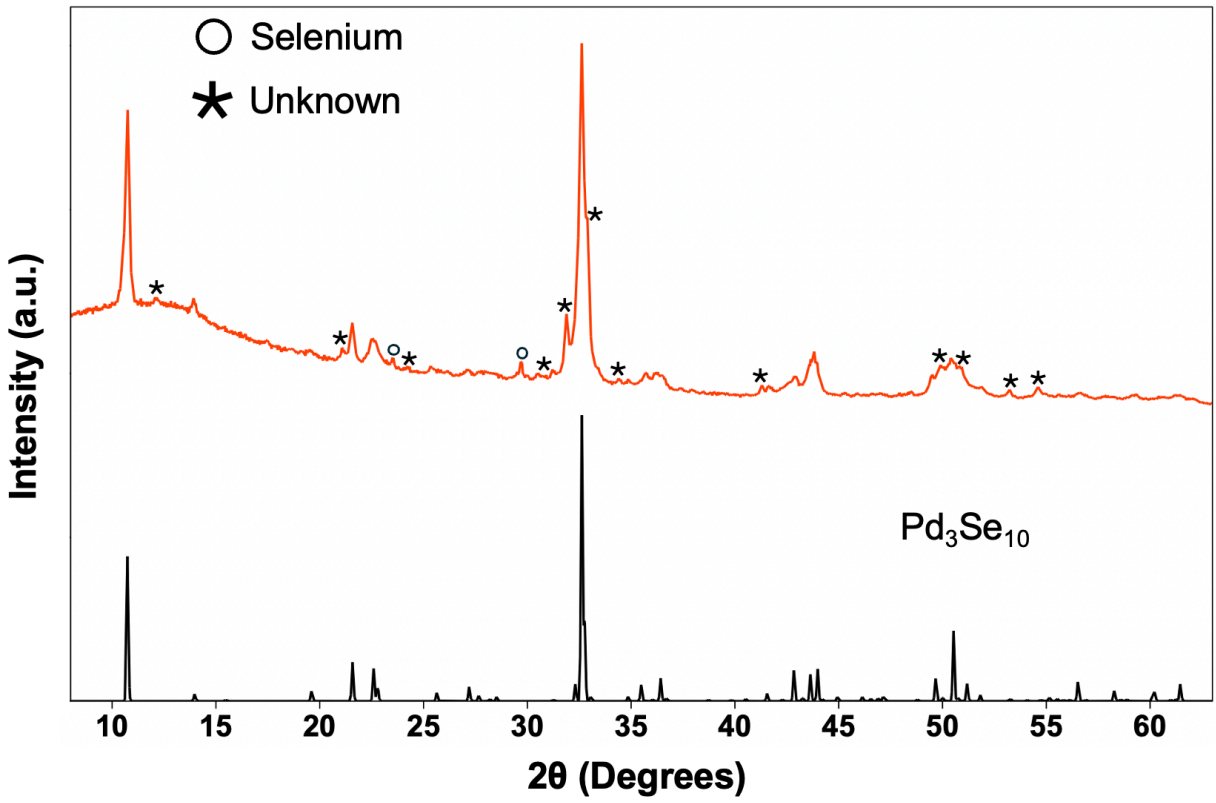

Figure S4. PXRD pattern (red) for the product of the 1 h reaction at 200 °C with a fast addition of the Na_2PdCl_4 precursor. The Pd_3Se_{10} reference pattern is shown in black. The circles indicate peaks corresponding to selenium and the asterisks indicate peaks corresponding to an unknown impurity. The broad peak around 15° in the PXRD pattern is due to the amorphous plastic sample holder used during data collection.

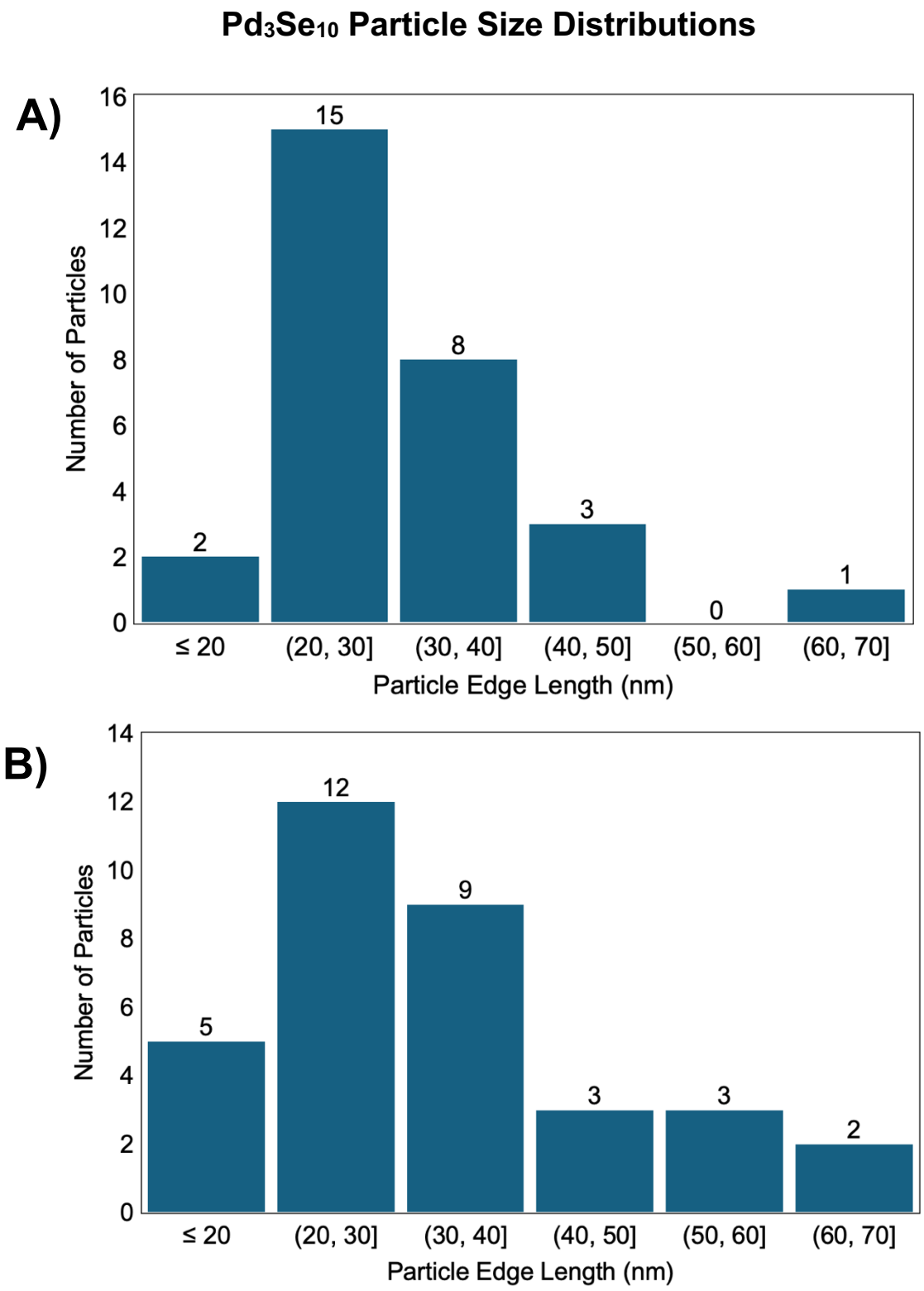

Figure S5. Pd_3Se_{10} particle size distributions measured using TEM. A) Distribution for the sample with an average 30 nm crystalline domain size as determined by the Scherrer equation. B) Distribution for the sample with an average 15 nm crystalline domain size as determined by the Scherrer equation.

Pd_3Se_{10} Selected Area Electron Diffraction (SAED) Indexing

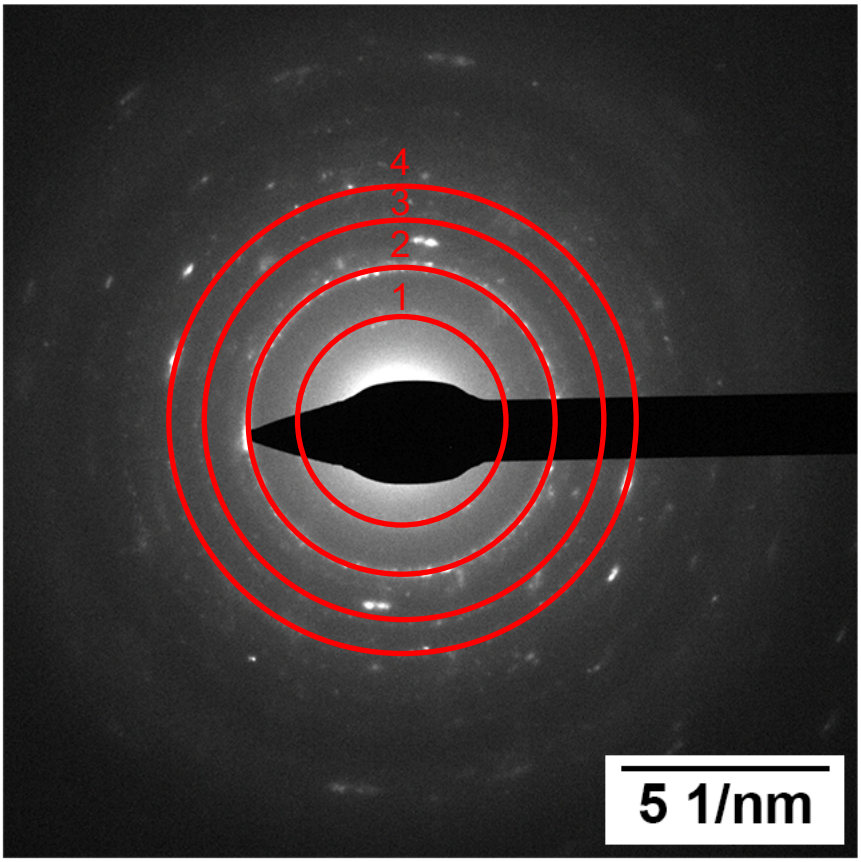

Figure S6. SAED Pattern of Pd_3Se_{10} with red circles indicating the rings used for indexing.

Table S6. Measured d-spacings for the SAED pattern of Pd_3Se_{10}.

Ring Number	Miller Index	Measured d-spacing from SAED pattern (Å)	Actual d-spacing from Pd_3Se_{10} crystal structure (Å)	Percent Difference between Measured and Actual d-spacings
1	(113)	3.96	3.93	0.76%
2	(303)	2.72	2.74	0.73%
3	(404)	2.05	2.06	0.49%
4	(330)	1.78	1.80	1.11%

Pd_3Se_{10} EDX Results

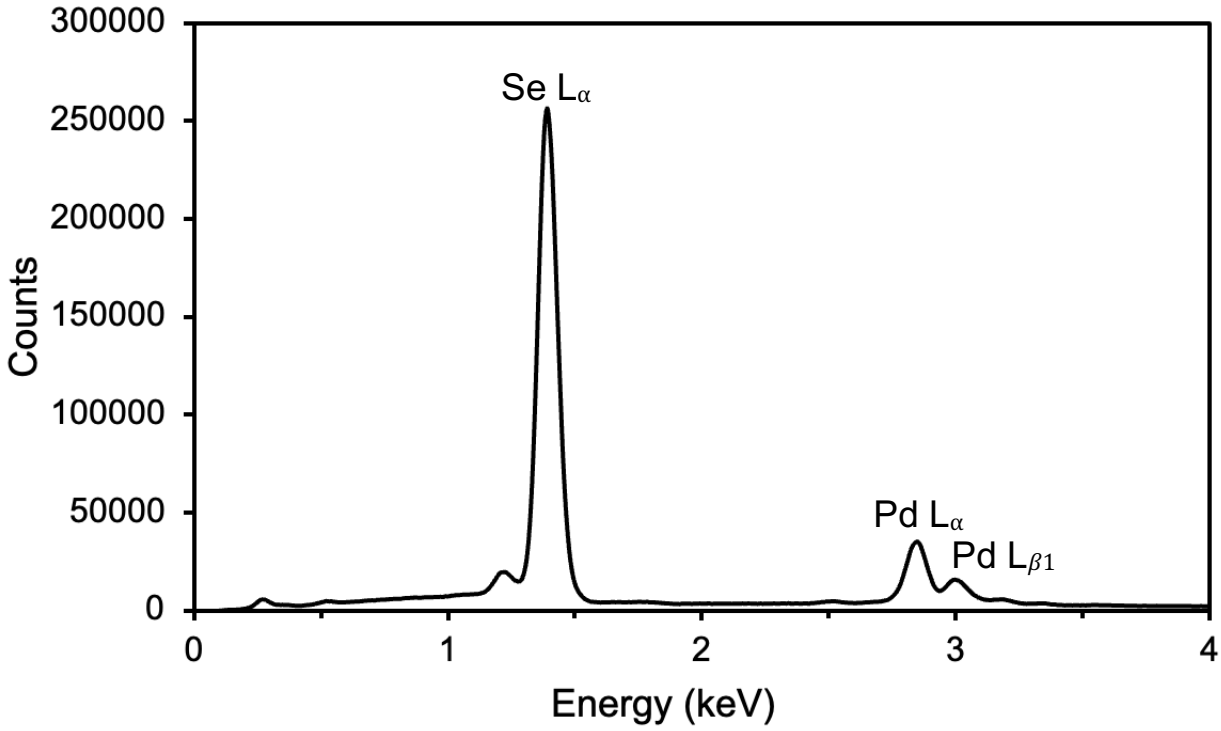

Figure S7. EDX spectrum for Pd_3Se_{10}.

Table S7. EDX quantification results for Pd_3Se_{10}.

Element	Se L	Pd L
Weight %	69.17	30.83
Atomic %	75.14	24.86
Error %	2.99	3.82

Raman Spectra Comparison of Palladium Selenide Phases

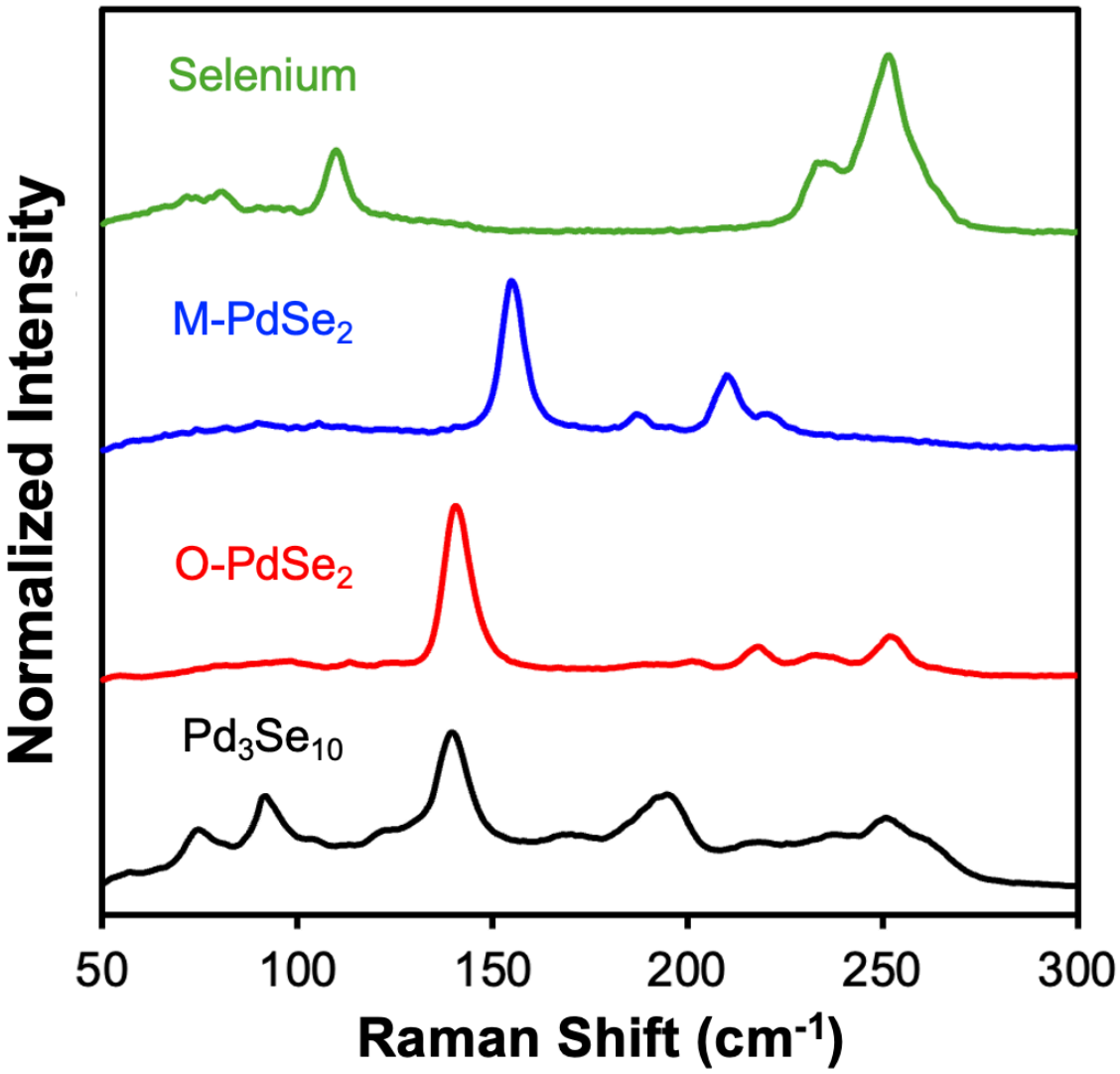

Figure S8. Raman spectra of crystalline Pd_3Se_{10}, orthorhombic $PdSe_2$ (O-$PdSe_2$), monoclinic $PdSe_2$ (M-$PdSe_2$), and selenium. O-$PdSe_2$ and M-$PdSe_2$ were prepared using previously described solution-phase methods.[3] For the selenium sample, a ground up selenium shot (Thermo Scientific, 99.999%) was used.

General Mechanism for Crystalline Pd_3Se_{10} Formation

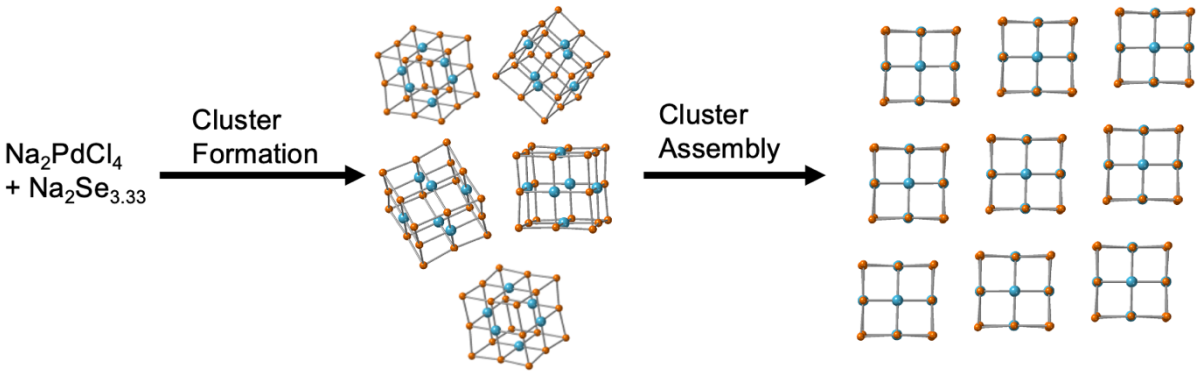

Figure S9. Schematic diagram of the proposed general mechanism of forming crystalline Pd_3Se_{10}. Pd atoms are blue and Se atoms are orange.

X-ray Diffraction Patterns for Crystalline Pd_3Se_{10} Before and After a 300 °C Heat Treatment

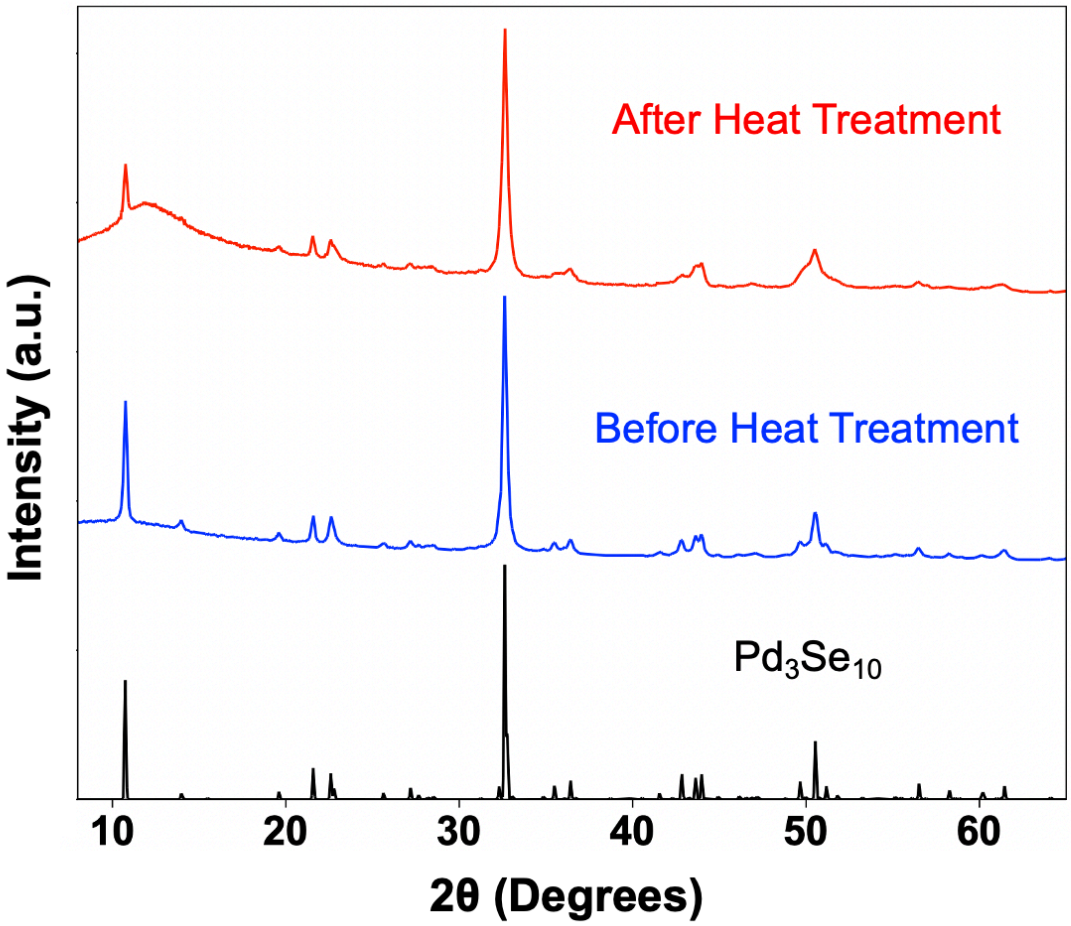

Figure S10. PXRD patterns of a crystalline Pd_3Se_{10} sample before and after a 300 °C heat treatment. The Pd_3Se_{10} powder was heated in a TGA instrument to 300 °C at a rate of 20 °C/min and cooled down to room temperature at the same rate. The broad peak around 15° in the PXRD pattern is due to the amorphous plastic sample holder used during data collection.

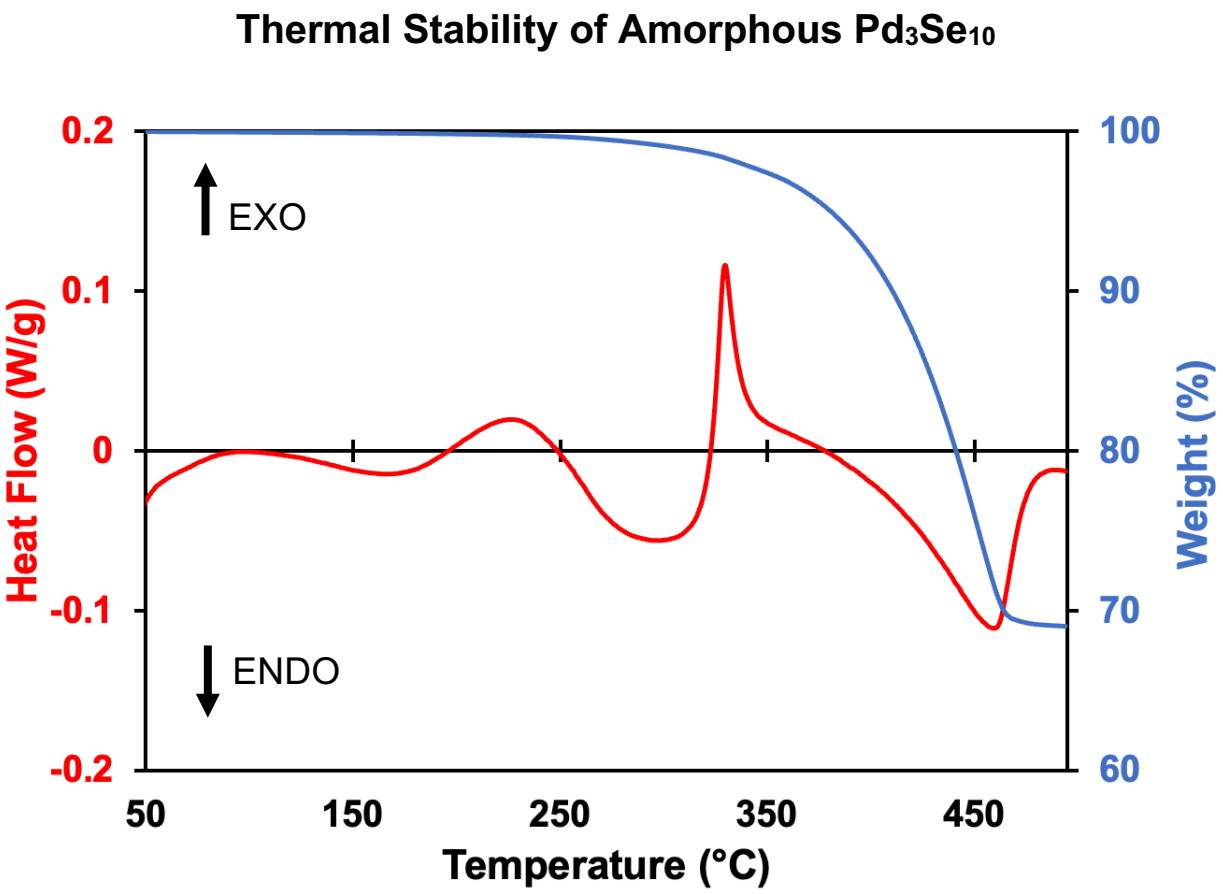

Figure S11.TGA-DSC data for the amorphous Pd_3Se_{10} sample synthesized at 150 °C. The sample was heated to 500 °C at a rate of 10 °C/min.

X-ray Diffraction Pattern for the Decomposition Product of Amorphous Pd_3Se_{10}

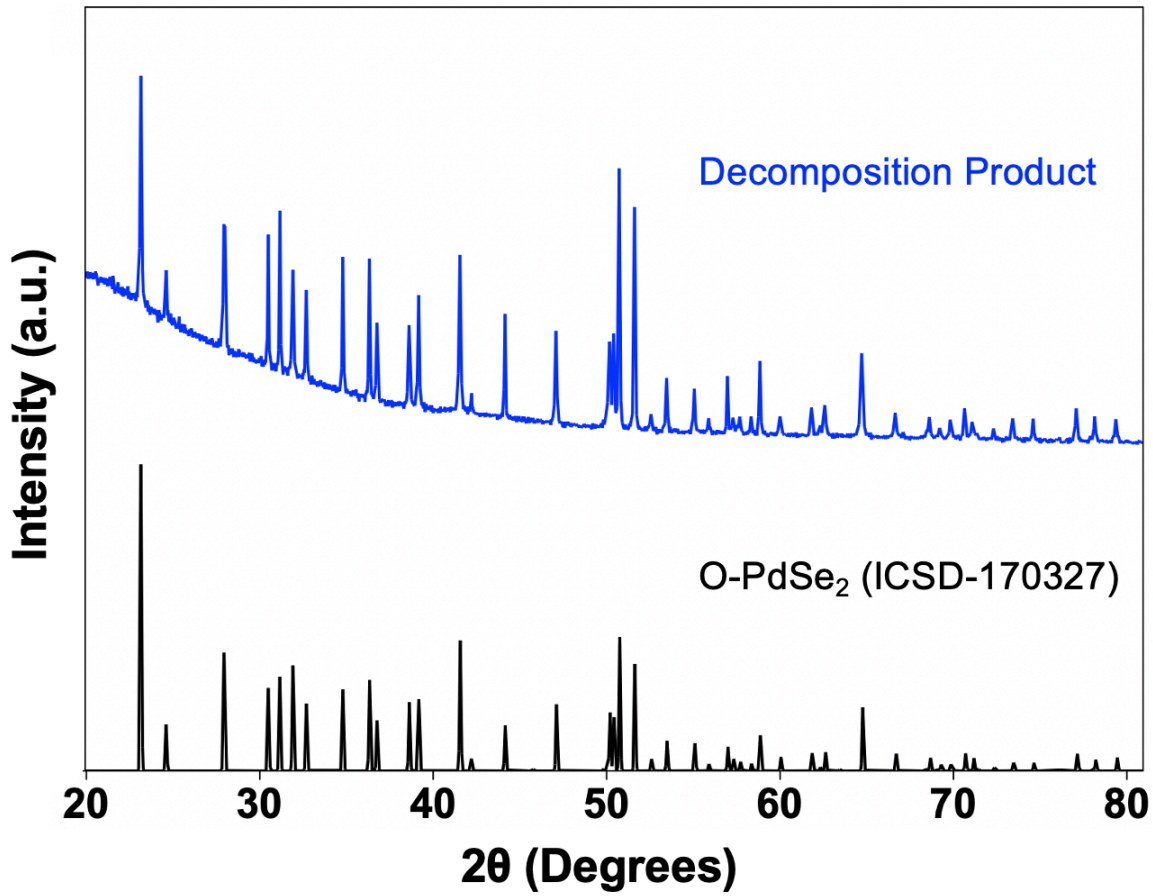

Figure S12. PXRD pattern of the product formed after the 500 °C heat treatment of the amorphous Pd_3Se_{10} sample.

Band Gap Determination Assuming a Direct Transition for Pd_3Se_{10} (30 nm size)

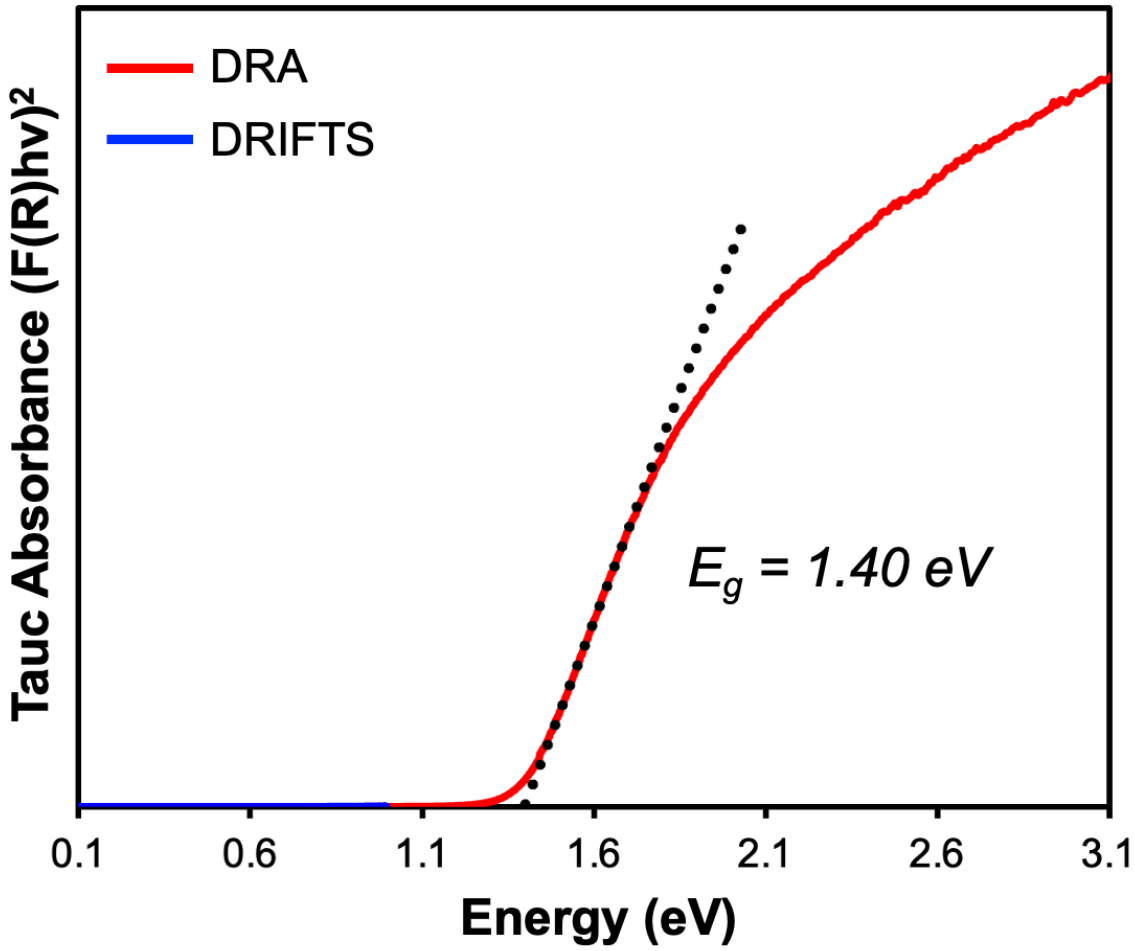

Figure S13. Tauc plot, assuming a direct transition, for the Pd_3Se_{10} sample with a crystalline domain size of 30 nm, as determined by the Scherrer equation.

Band Gap Determination for Crystalline Pd_3Se_{10} (15 nm size)

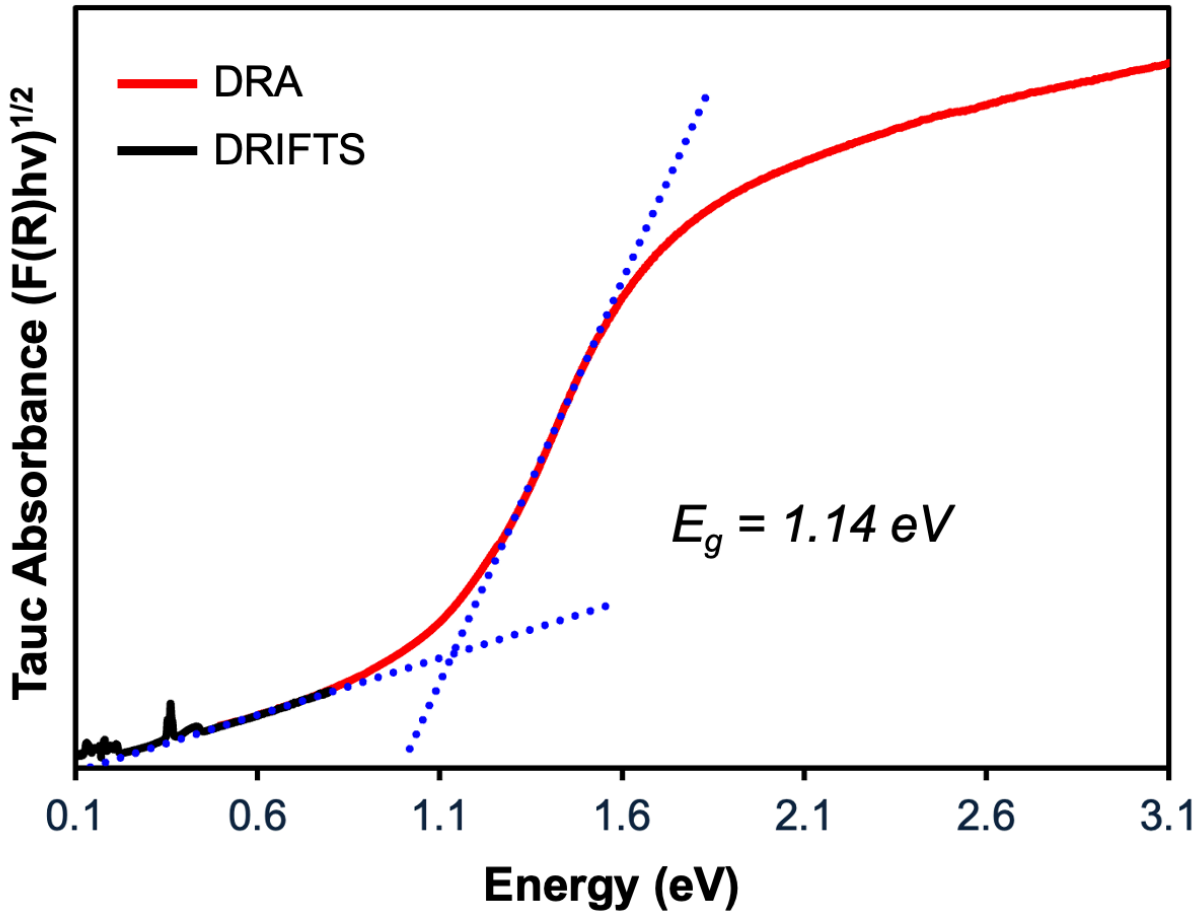

Figure S14. Tauc plot, assuming an indirect transition, for the Pd_3Se_{10} sample with a crystalline domain size of 15 nm, as determined by the Scherrer equation.

Urbach Energy Equations

For the Urbach tail region, or the energy region slightly below than the band gap, the optical absorption coefficient can be modeled using the equation below.[4-6]

$$\alpha = \alpha_0 \exp\left(\frac{E - E_g}{E_U}\right)$$

In the above equation, α is the optical absorption coefficient, α_0 is a constant, E is photon energy, E_g is the optical band gap, and E_U is the Urbach energy. If the natural logarithm of both sides of the equation is taken, it can be rewritten as:

$$\ln(\alpha) = \left(\frac{1}{E_U}\right) E + C$$

The expression shown above conveniently takes the form of a linear equation (y = mx + b) where y is $\ln(\alpha)$, x is E, and the slope is $1/E_U$. C is a constant that can be described by a mathematical expression consisting of α_0, E_g, and E_u. To extract the Urbach energy, a plot of $\ln(\alpha)$ versus E needs to be made. Then, a line should be fit to the Urbach tail region of the plot and the inverse of the slope of the line will be E_u.[7]

In our case, we have a Kubelka-Munk absorption plot instead of an absorption coefficient plot. Since Kubelka-Munk absorbance (F(R)) is proportional to the absorption coefficient,[8] we can replace α with F(R) to get the following expression:

$$\ln\big(F(R)\big) = \left(\frac{1}{E_U}\right) E + C$$

Urbach energy can be extracted from a plot of ln(F(R)) versus E in an analogous way to what was described above.[8-11] Technically, we should not consider this Urbach energy to be equivalent to an Urbach energy determined from an absorption coefficient plot, since the two values would have different units.[12] However, obtaining Urbach energies from Kubelka-Munk absorption plots still allows for a quantitative comparison between different samples.

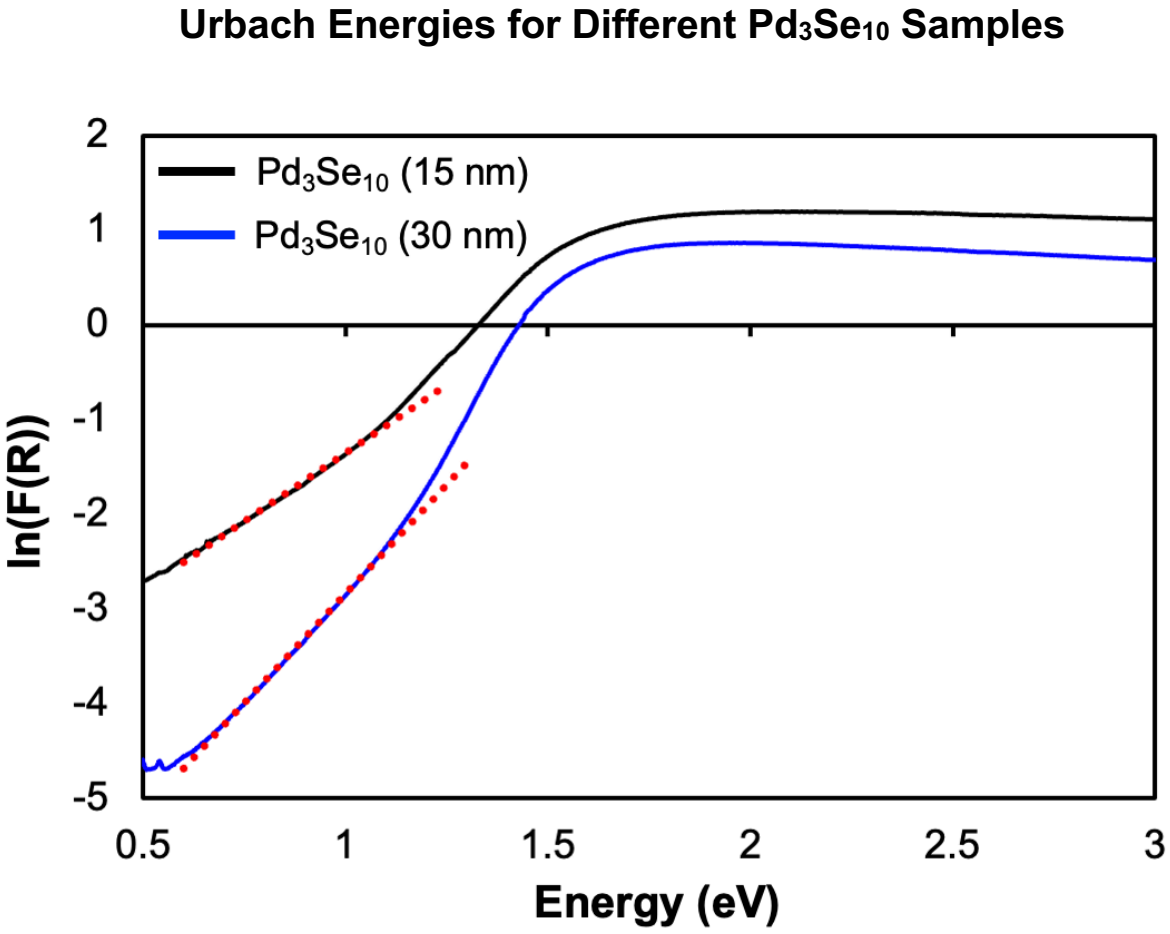

Figure S15. Plot of the natural logarithm of the Kubelka-Munk absorbance (F(R)) versus energy that was used to extract Urbach energies. Urbach energies were determined for the crystalline Pd_3Se_{10} samples with domain sizes of 30 nm and 15 nm, as determined by the Scherrer equation. For the linear fits (red dotted lines) for both samples, only data in the 0.7-1.1 eV energy range was used.

Table S8. Urbach energies for Pd_3Se_{10} samples with different crystalline domain sizes.

Domain Size (nm)	Slope of linear fit (eV^{-1})	Urbach Energy (eV)
15 nm	2.89	0.346
30 nm	4.61	0.217

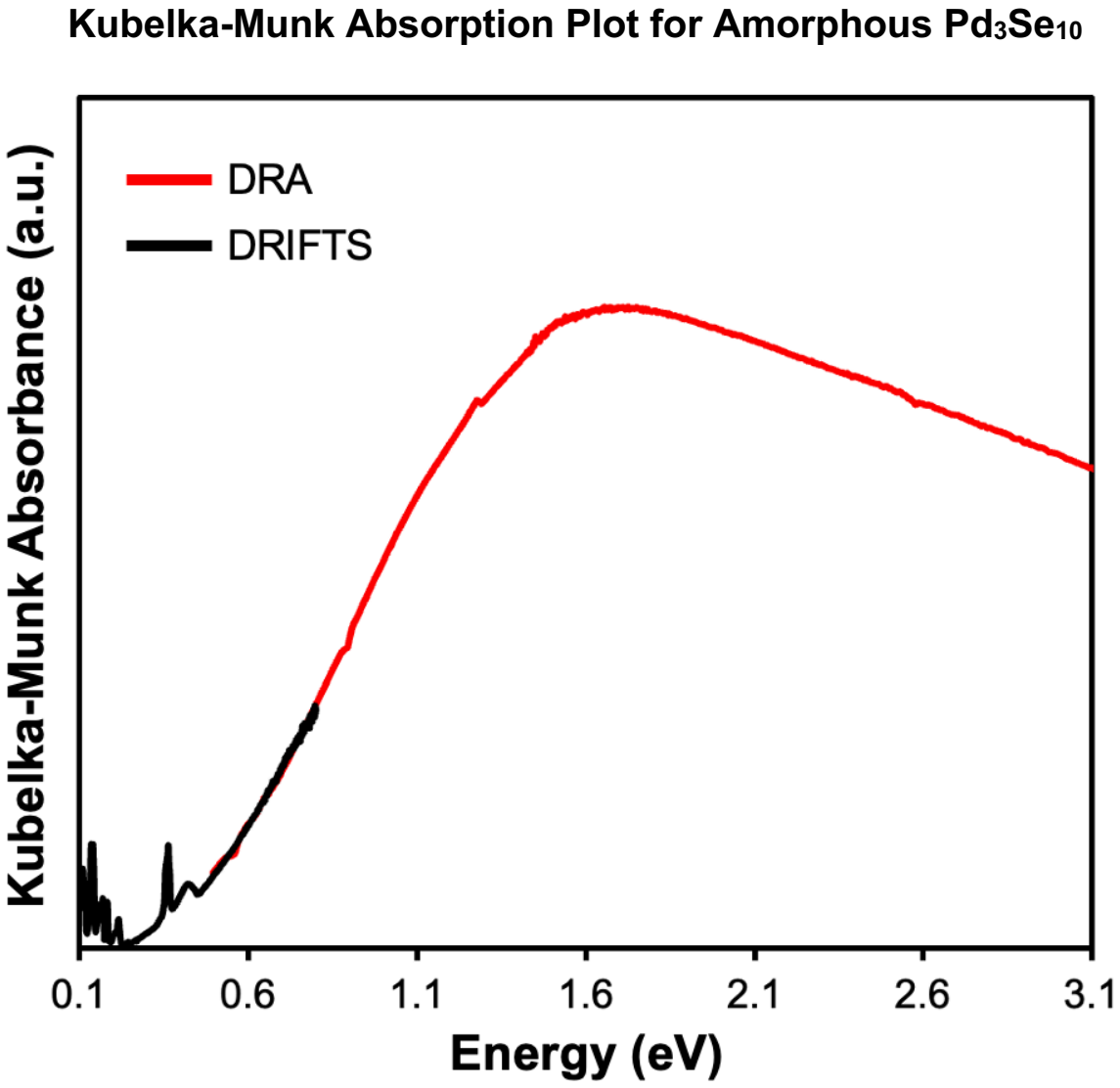

Figure S16. Kubelka-Munk absorption plot for the amorphous Pd_3Se_{10} sample synthesized at 150 °C.

References:

1. V. P. Böttcher, *Z. Anorg. Allg. Chem*, 1977, **432**, 167-172.
2. V. P. Böttcher, *Z. Anorg. Allg. Chem*, 1980, **461**, 13-21.
3. C. T. Irvine, N. Hoefer, M. J. Moser, R. A. Nelson, D. W. McComb and J. E. Goldberger, *Chem. Mater.*, 2023, **35**, 4404-4411.
4. M. Li, P. Huang and H. Zhong, *J. Phys. Chem. Lett*, 2023, **14**, 1592-1603.
5. J. Klein, L. Kampermann, B. Mockenhaupt, M. Behrens, J. Strunk and G. Bacher, *Adv. Funct. Mater.*, 2023, **33**, 2304523.
6. A. Kumar, O. V. Rambadey and P. R. Sagdeo, *J. Phys. Chem. C*, 2021, **125**, 7378-7383.
7. D. Kandi, S. Martha, A. Thirumurugan and K. M. Parida, *ACS Omega*, 2017, **2**, 9040-9056.
8. K. Kumar, O. V. Rambadey and P. R. Sagdeo, *J. Phys. Chem. C*, 2023, **127**, 22164-22176.
9. Y. Liu, J. Wei, Y. Guo, T. Yang and Z. Xu, *RSC Adv.*, 2016, **6**, 96563-96572.
10. D. Mora-Herrera and M. Pal, *Appl. Phys. A*, 2022, **128**, 1008.
11. H. A. N. Dharmagunawardhane, A. James, Q. Wu, W. R. Woerner, R. M. Palomino, A. Sinclair, A. Orlov and J. B. Parise, *RSC Adv.*, 2018, **8**, 8976-8982.
12. M. Abdi-Jalebi, M. Ibrahim Dar, A. Sadhanala, E. M. J. Johansson and M. Pazoki, in *Characterization Techniques for Perovskite Solar Cell Materials*, eds. M. Pazoki, A. Hagfeldt and T. Edvinsson, Elsevier, 2020, pp. 49-79.